CorSegRec: A Topology-Preserving Scheme for Extracting Fully-Connected Coronary Arteries from CT Angiography

Yuehui Qiu[1], Zihan Li[3], Yining Wang[4], Pei Dong[6], Dijia Wu[5,6], Xinnian Yang[7], Qingqi Hong[2,8(✉)], and Dinggang Shen[5,6(✉)]

[1] School of Informatics, Xiamen University, Xiamen, China
[2] Department of Digital Media Technology, Xiamen University, Xiamen, China
hongqq@xmu.edu.cn
[3] Univeristy of Washington, Seattle, USA
[4] Peking Union Medical College Hospital, Beijing, China
[5] School of Biomedical Engineering, ShanghaiTech University, Shanghai, China
[6] Shanghai United Imaging Intelligence Co., Ltd., Shanghai, China
dgshen@shanghaitech.edu.cn
[7] City University of Hong Kong, Hong Kong, China
[8] Hong Kong Centre for Cerebro-Cardiovascular Health Engineering (COCHE), Hong Kong, China

Abstract. Accurate extraction of coronary arteries from coronary computed tomography angiography (CCTA) is a prerequisite for the computer-aided diagnosis of coronary artery disease (CAD). Deep learning-based methods can achieve automatic segmentation of vasculatures, but few of them focus on the connectivity and completeness of the coronary tree. In this paper, we propose CorSegRec, a topology-preserving scheme for extracting fully-connected coronary artery, which integrates image segmentation, centerline reconnection, and geometry reconstruction. First, we employ a new centerline enhanced loss in the segmentation process. Second, for the broken vessel segments, we propose a regularized walk algorithm, by integrating distance, probabilities predicted by centerline classifier, and cosine similarity to reconnect centerlines. Third, we apply level-set segmentation and implicit modeling techniques to reconstruct the geometric model of the missing vessels. Experiment results on two datasets demonstrate that the proposed method outperforms other methods with better volumetric scores and higher vascular connectivity. Code will be available at https://github.com/YH-Qiu/CorSegRec.

Keywords: Coronary artery extraction · Centerline reconnection · Geometry reconstruction · Regularized walk

1 Introduction

Coronary computed tomographic angiography (CCTA) is a well-established non-invasive imaging modality to diagnose coronary artery disease (CAD) which is a

H. Greenspan et al. (Eds.): MICCAI 2023, LNCS 14222, pp. 670–680, 2023.
https://doi.org/10.1007/978-3-031-43898-1_64

common disease with increasing prevalence worldwide [15]. Accurate extraction of coronary arteries from CCTA can assist doctors in diagnosis and treatment of CAD [16].

Manual segmentation of coronary arteries is time-consuming and expensive. As a result, multiple traditional methods based on image processing techniques have been developed over the years to automatically or semi-automatically segment coronary arteries [1,2]. With the rapid development of deep learning, more methods have been proposed to automatically extract coronary arteries which show better scalability and higher accuracy [18–20,23]. Wolterink et al. [19] used graph convolutional networks to predict vertices in the luminal surface mesh. Zhu et al. [23] designed a multi-scale CNN for thin artery segmentation. Wang et al. [18] aggregated local features on point clouds to remove irrelevant vessels. Zhang et al. [20] captured anotamical dependence and hierarchical topology representations for accurate segmentation. Recent studies on coronary artery segmentation gradually pay attention to extracting thin structures [19,23] or removing false vessels [18], but few of them [20] focus on both two aspects.

In spite of reasonably good performance achieved by deep learning-based methods, there are still often some disconnected segments in segmentation results, which may be the mispredicted vessels, or may be caused by the presence of artifacts, stenosis, plaques, and occlusions [9]. Vascular connectivity has an important impact on the screening of vascular lesions. Several studies have been carried out to reconnect the broken vessels in 2D [7,11,13] and 3D [3,6], including coronary arteries. All these studies integrate both local vesselness details and geometric priors in vessel reconnection process. But there is no strategy which is specially designed for 3D coronary artery reconnection and show capability to handle complex disconnections and obtain the complete coronary tree to our knowledge.

In this paper, we propose a topology-preserving scheme for the extraction of fully-connected coronary arteries, integrating image segmentation, centerline reconnection, and geometry reconstruction. Our major contributions are as follows: 1) We design a new centerline enhanced loss for coronary artery segmentation; 2) We propose the distance probability cosine (DPC) regularized walk algorithm to reconnect the broken centerlines; 3) We use a reconstruction method based on 2D level-set model and 3D implicit modeling technique to reconstruct vascular model along the stitched centerlines.

2 Method

As shown in Fig. 1, the proposed CorSegRec consists of three stages: vascular segmentation stage, vascular reconnection stage and vascular reconstruction stage. Firstly, CCTA images are fed into a vascular segmentation network (e.g. nnU-Net [8]) and trained with the proposed centerline enhanced loss to obtain the initial segmentation result. Then, we reconnect the broken centerlines with the proposed distance, probability, and cosine similarity (DPC) regularized walk algorithm. Finally, we reconstruct the broken vascular model along the

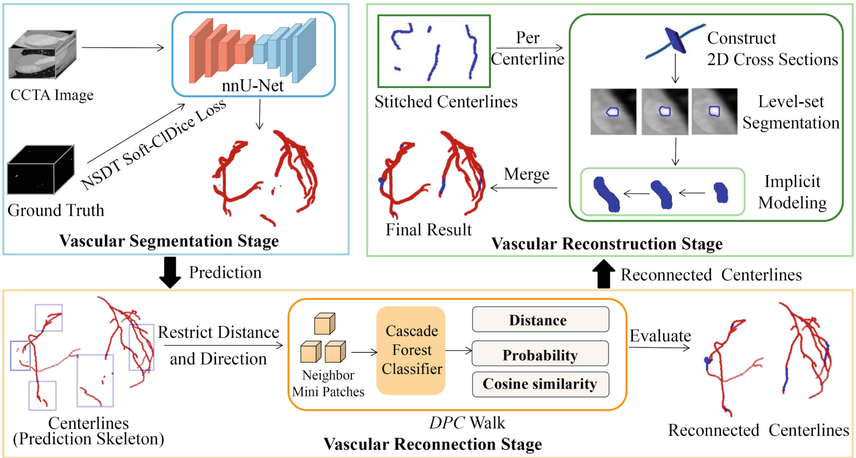

Fig. 1. Overview of CorSegRec.

stitched cenerlines by integrating level-set segmentation and implicit modeling techniques, and obtain the fully-connected coronary tree.

2.1 Vascular Segmentation Based on NSDT Soft-ClDice Loss

Shit et al. [17] proposed Soft-ClDice for tubular structure segmentation, in which vessel voxels on skeleton and near wall are assigned with the same weight. However, the centerlines of vessels contain significant topology information. Therefore, we calculate the normalized distance from foreground voxels in masks to skeletons to increase the weights of vessel skeletons. In addition, the skeletons of vessels with different radii are increased to the same weight, which will be beneficial for detecting thin vascular structures. As a result, the network will be more sensitive to vascular topology, and thus detect more hard-to-segment vessels and improve the potential of reconnection. The proposed Normalized Skeleton Distance Transform (NSDT) Soft-ClDice loss is denoted as $\mathcal{L}_{dscl}$ and calculated as follows:

$$\mathcal{L}_{dscl} = 1 - 2 \times \frac{\text{Tprec}^*(S_P, V_L) \times \text{Tsens}^*(S_L, V_P)}{\text{Tprec}^*(S_P, V_L) + \text{Tsens}^*(S_L, V_P)} \tag{1}$$

$$\text{Tprec}^*(S_P, V_L) = \frac{|(S_P \circ NSDT_P \circ V_P) \circ NSDT_L|}{|(S_P \circ NSDT_P) \circ (S_P \circ NSDT_P)|} \tag{2}$$

$$\text{Tsens}^*(S_L, V_P) = \frac{|(S_L \circ NSDT_L) \circ (NSDT_P \circ V_P)|}{|(S_L \circ NSDT_L) \circ (S_L \circ NSDT_L)|} \tag{3}$$

$$NSDT_L = \begin{cases} \inf\limits_{y \in (S_L)_{in}} \frac{R}{\|x-y\|_2+1}, & x \in (V_L)_{in} \\ 0, & otherwise \end{cases} \tag{4}$$

where V_L and V_P represent true mask and real-valued probabilistic prediction, while S_L, S_P represent their skeletons, and $NSDT_L$, $NSDT_P$ represent their normalized skeleton distance transform masks. $\circ$ is the Hadamard product. The first and second parts of numerator in Eq. (2) and Eq. (3) represent skeletons and masks with NSDT (and probability) values respectively. In Eq. (4), $_{in}$ represents foreground, $\|x-y\|_2$ calculates the Euclidean distance between voxel x and y. R is the amplification parameter and set to the maximum skeleton distance in one case.

We combine Soft-Dice loss ($\mathcal{L}_{dc}$) and $\mathcal{L}_{dscl}$ in training, and get the final loss:

$$\mathcal{L}_{dc\&dscl} = (1-\gamma)\mathcal{L}_{dc} + \gamma\mathcal{L}_{dscl} \tag{5}$$

where γ is the balancing weight and set to 0.5 empirically.

2.2 Vascular Reconnection Based on *DPC* Walk

To improve the connectivity of the segmented coronary arteries, we propose the *DPC* walk algorithm to reconnect the disconnected vascular centerlines.

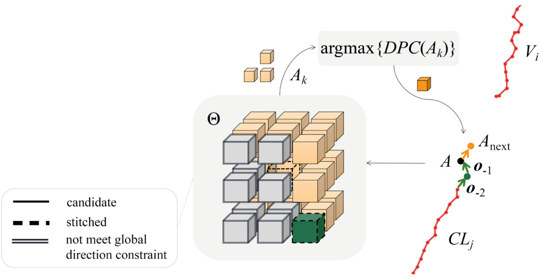

Fig. 2. Illustration of *DPC* Walk. The red lines represent two centerlines to connect. A is the current point. The green arrows represent offset vectors of the last two stitched points ($\boldsymbol{o}_{-1}$, $\boldsymbol{o}_{-2}$). In A's neighbors (Θ), the green, grey, light yellow cubes represent the stitched points, points not meeting global direction constraint and candidate points respectively. The candidate with max *DPC* is A_{next} (in dark yellow). (Color figure online)

First, centerlines are extracted from predictions. We refer to the centerlines of the two biggest connected components as $V_i(i = 1, 2, ...)$ and other broken centerlines as $CL_j(j = 1, 2, ...)$. V_i consists of a sequence of points $(p_1, p_2, ..., p_m)$ where p_1 represents the head and p_m represents the tail, while CL_j is represented by $(q_1, q_2, ..., q_n)$. Then we select candidate branches for CL_j by distance and direction.

To connect CL_j to candidate V_i, we iteratively make locally optimal decisions based on distance (D), centerline probability (P) and cosine similarity (C). The goal is to identify a potential path from the head of CL_j to the tail of V_i. In general, if the current point of walker is A, then its 26-connected neighbors are denoted as $\Theta = \{A_k | k = 1, 2, ..26\}$, which form a cube sized $3 \times 3 \times 3$ (see Fig. 2). The D, P and C for each neighbor point A_k are calculated as follows:

$$D(A_k) = -\|A_k - p_m\|_2 \tag{6}$$

$$P(A_k) = CFC.predict\_proba(flatten(patch(A_k))) \tag{7}$$

$$C(A_k) = \cos(\boldsymbol{o}_k, \boldsymbol{o}_{-1}) + \cos(\boldsymbol{o}_k, \boldsymbol{o}_{-2}) \tag{8}$$

where D is the inverse distance between A_k and p_m, P is the probability that A_k is on the centerline, and C is the cosine similarities between A_k's offset vector ($\boldsymbol{o}_k$) and the offset vectors of the last two stitched points ($\boldsymbol{o}_{-1}$, $\boldsymbol{o}_{-2}$). To obtain P, we first train a centerline binary classifier on mini patch level using cascade forest classifier (CFC) [22] due to its few hyper parameters and high training efficiency. While predicting P for A_k, we create a patch of size $l \times l \times l$ centered at A_k. We then flatten the patch and input it into CFC.

D, P and C are added up, with P of a weight denoted as ω, which is generally set to 5 but magnified ten-fold in environment of extremely low P. When the direction of $\boldsymbol{o}_{-1}$ and $\boldsymbol{o}_{-2}$ is too close, we avoid calculating C to prevent a straight line in walk. The calculation of DPC is defined as follows:

$$DPC(A_k) = \begin{cases} D(A_k) + \omega P(A_k) + C(A_k), & \cos(\boldsymbol{o}_{-1}, \boldsymbol{o}_{-2}) \le \frac{1}{2} \\ D(A_k) + \omega P(A_k), & otherwise \end{cases} \tag{9}$$

The global direction is a vector from q_1 to p_m, denoted as $\boldsymbol{v}$. And the cosine similarity of candidate $\boldsymbol{o}_k$ and $\boldsymbol{v}$ should be greater than 0. We then select the next point (A_{next}) with the largest DPC from the current point A (see Fig. 2):

$$A_{next} = \underset{A_k \in \Theta, \cos(\boldsymbol{o}_k, \boldsymbol{v}) \ge 0}{\arg\max} \{DPC(A_k)\} \tag{10}$$

The reconnection process ends abnormally by steps beyond the limit or continuous low probabilities. If A arrives at p_m, we then analyse the probability sequences and filter out unstable reconnections. Finally, we remove the vascular segments reconnected unsuccessfully and obtain reconnected centerlines.

2.3 Vascular Reconstruction Based on Level-Set Segmentation and Implicit Modeling

The task of coronary reconstruction stage is to reconstruct the vascular model along the stitched centerlines and obtain a coronary artery tree with full connectivity.

Firstly, we construct cross-section profiles perpendicular to the stitched centerlines, and extract the corresponding vessel contours using level-set model. We propose a Self-adaptive Local Hybrid level-set model, which can automatically calculate the dynamic threshold using the local region information to act as the lower bound of target object. The energy function is defined as follows:

$$E^{SLH}(\phi) = \alpha \int_{\Omega} (I(x) - \mu(x, \phi)) H(\phi) dx + \beta \int_{\Omega} g(|\nabla I(x)|) \, |\nabla H(\phi)| \, dx \tag{11}$$

where α and β are pre-set weights, I is image, ϕ is the contour represented by the level-set method, $g(*)$ is monotone decreasing function of $[0, \infty] \rightarrow R+$, and $H(\phi)$ is Heaviside function. $\mu(x, \phi)$ is the automatically calculated local threshold, and calculated as follows:

$$\mu(x, \phi) = \frac{[I(x)H(\phi)] * K_\sigma(x)}{H(\phi) * K_\sigma(x)} \tag{12}$$

where $K_\sigma(x)$ is a truncated Gaussian window sized $(4k+1) \times (4k+1)$. k is the largest integer smaller than the standard deviation.

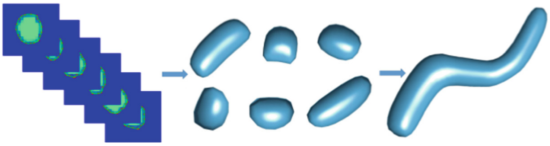

Fig. 3. Illustration of tubular structure modeling based on implicit spline functions.

Secondly, the extracted vessel contours are represented as 2D Partial Shape-Preserving Spline (PSPS) functions [10], and different cross-section profiles are weighted and extruded into 3D vessel models along the centerline using the 1D PSPS basis functions (Fig. 3). Finally, these reconstructed 3D vessel models are merged with the original vessel branches to ultimately obtain the fully-connected coronary artery tree.

3 Experiments

3.1 Setup

Dataset. We validate our approach on two datasets. The first dataset is public available from the MICCAI 2020 Automated Segmentation of Coronary Arteries (ASOCA) challenge[1] [4,5]. ASOCA includes 60 CCTA images, 40 for training and 20 for testing, half of which are patients with CAD. The second dataset named PDSCA is from reference [20], including 50 CCTAs, which is evaluated by five-fold cross-validation for fair comparison.

Evaluation Metric. The quantitative results are reported using Dice similarity coefficient (Dice), Hausdorff Distance (HD) and Overlap (OV). Besides, Reconnection Accuracy (RecAcc) is defined to evaluate how successful *DPC* Walk is to reconnect the broken vessels by calculating directly on centerlines involved in reconnection and removal:

$$\text{RecAcc} = \frac{(\text{TP}_\text{b} + \text{TP}_\text{s}) + \text{TN}_\text{b}}{(\text{TP}_\text{b} + \text{TP}_\text{s}) + \text{TN}_\text{b} + (\text{FP}_\text{b} + \text{FP}_\text{s}) + \text{FN}_\text{b}} \tag{13}$$

[1] https://asoca.grand-challenge.org/.

where $_\mathrm{b}$ and $_\mathrm{s}$ represent the broken and stitched centerlines respectively. For the points on these centerlines, we label them by comparing the reconnected centerlines with ground truth. Similarly, we obtain Reconnection Sensitivity (RecSen) and Reconnection Specificity (RecSpe):

$$\mathrm{RecSen} = \frac{\mathrm{TP_b} + \mathrm{TP_s}}{(\mathrm{TP_b} + \mathrm{TP_s}) + \mathrm{FN_b}} \quad \mathrm{RecSpe} = \frac{\mathrm{TN_b}}{\mathrm{TN_b} + (\mathrm{FP_b} + \mathrm{FP_s})} \tag{14}$$

3.2 Implementation Details

1) We trained 3d_fullres version of nnU-Net [8] as baseline in environment of NVIDIA GETFORCE GTX 1080Ti, Python 3.7.11 and PyTorch 1.7.1, only loss function modified. 2) We used CascadeForestClassifier [22] implemented in Python deepforest library as centerline classifier. The length parameter l was set to 7, while for thick vessels it was 15 and finally unified to 7 by maxpool. We ramdomly sampled mini image patches centered at voxels on training set with a ratio 1:4 for positive and negative samples. The validation accuracy reached 86% and 94% for two categories respectively.

3.3 Comparison with State-of-the-Art Methods

We performed quantitative comparisons with some advanced deep learning-based segmentation methods on ASOCA and PDSCA as presented in Table 1 and Table 2.

For ASOCA, our CorSegRec has better performance in Dice and HD compared with other methods using vanilla 2D or 3D U-Net, and nnU-Net [8] with pre-processing, network improvement or post-processing. It proves CorSegRec has stronger ability in extracting coronary arteries compared with some methods of vascular enhancing and removal.

For PDSCA, our approach shows significant improvements in Dice and HD compared with ResU-Net [12] and MPSPNet [23]. The rest of methods pay attention to the structures of objects in segmentation [14,17,20]. Differently, we focus on learning useful information from probability and direction to reconnect the broken vessels and get the best results.

3.4 Ablation Study

Ablation Study on Components of *DPC* Walk. We conducted several experiments by combining different subsets of D, P, and C. As shown in Table 3, DPC Walk outperforms the others in terms of RecAcc, RecSen and OV. Our focus is to extract a complete coronary tree by emphasizing connection rather than removal, hence the RecSpe is relatively low. The walk without P yielded the worst results, indicating that P is the critical component of the DPC Walk algorithm. The ranking of PC and DP is close, as both have the crucial P. PC Walk lacks guidance to the destination and may encounter difficulties in long-distance reconnections, whereas DP Walk is unable to handle situations when D or P dominates. Overall, DPC Walk is the optimal choice.

Table 1. Quantitative comparison with the state-of-the-art methods on ASOCA. (mean ± std, best results in **bold**). (* The methods and results are reported in [4] for reference).

Method	Dice (%)	HD (mm)
2D Res SE U-Net*	84.00 ± 5.00	2.34 ± 2.92
3D Vessel U-Net*	86.00 ± 7.00	6.22 ± 15.52
Hessian nnU-Net*	87.00 ± 5.00	6.57 ± 14.27
scale nnU-Net*	87.00 ± 4.00	4.16 ± 7.30
UGAN [21]	87.50 ± 4.30	8.92 ± 15.8
CorSegRec	$\mathbf{89.46 \pm 3.39}$	$\mathbf{1.89 \pm 3.37}$

Table 2. Quantitative comparison with the state-of-the-art methods on PDSCA. (mean ± std, best results in **bold**).

Method	Dice (%)	HD (mm)
ResU-Net [12]	70.25 ± 1.46	9.33 ± 0.22
MPSPNet [23]	73.60 ± 1.17	7.08 ± 0.24
CS^2-Net [14]	76.53 ± 1.29	7.33 ± 0.31
clDice [17]	76.72 ± 0.86	6.29 ± 0.18
PLF [20]	80.36 ± 0.93	6.50 ± 0.15
CorSegRec	$\mathbf{83.29 \pm 3.47}$	$\mathbf{2.52 \pm 3.68}$

Table 3. Ablation Study on components of *DPC* Walk (mean ± std, best results in **bold**). RecAcc, RecSen and RecSpe were calculated at dataset level, no std.

Dataset	Method	RecAcc (%)	RecSen (%)	RecSpe (%)	OV (%)
ASOCA	CorSegRec w/o *DPC*	–	–	–	83.38 ± 7.23
	CorSegRec w/ *DPC*	**90.27**	**97.69**	78.57	$\mathbf{87.33 \pm 6.40}$
	CorSegRec w/ *DP*	82.50	84.49	79.45	86.50 ± 6.87
	CorSegRec w/ *PC*	75.67	69.86	85.43	84.93 ± 9.26
	CorSegRec w/ *DC*	50.17	8.58	**93.32**	81.19 ± 12.21
PDSCA	CorSegRec w/o *DPC*	–	–	–	86.96 ± 4.78
	CorSegRec w/ *DPC*	**79.66**	**88.44**	72.25	$\mathbf{90.29 \pm 3.54}$
	CorSegRec w/ *DP*	74.21	80.81	68.89	89.84 ± 4.18
	CorSegRec w/ *PC*	76.23	63.93	86.27	89.58 ± 4.40
	CorSegRec w/ *DC*	63.33	18.57	**93.59**	87.63 ± 4.97

Ablation Study on Vascular Reconstruction. Figure 4 presents the evaluation of initial segmentation and final results using Dice (orange lines with a left y-axis) and HD (green bars with a right y-axis). The complete CorSegRec scheme achieves superior results. As shown in Fig. 5, most broken segments are correctly connected to the two largest components after reconstruction. Moreover, the reconstructed vessel models have similar appearance to the ground truth.

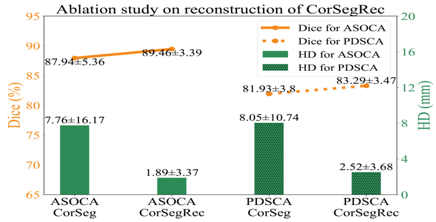

Fig. 4. Ablation study on the reconstruction of CorSegRec. CorSeg/CorSegRec represent the proposed method without/with model reconstruction respectively. The texts around represent mean ± std. (Color figure online)

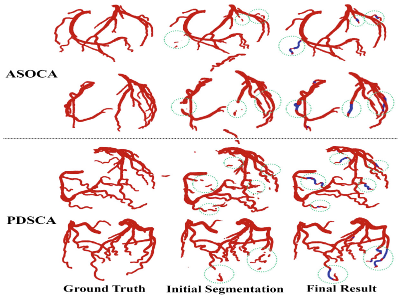

Fig. 5. Comparison of the initial segmentation and final results. The green circles highlight most broken regions. (blue: the reconstructed vessel models) (Color figure online)

4 Conclusion

In this paper, we present a new topology-preserving scheme called CorSegRec to extract fully-connected coronary arteries from CCTA. Our approach combines coronary artery segmentation, centerline reconnection, and coronary model reconstruction. Notably, the proposed *DPC* Walk algorithm can remove most false positive segments and effectively track and connect some arteries hard-to-segment. Experiment results on two CCTA datasets demonstrate that our method can achieve better connected and more accurate coronary artery extraction compared to other methods.

Acknowledgments. This work was supported in part by the Natural Science Foundation of Fujian Province of China (No. 2020J01006), the Open Project Program of State Key Laboratory of Virtual Reality Technology and Systems, Beihang University (No. VRLAB2022AC04), National Natural Science Foundation of China (No. 62131015), Beijing Natural Science Foundation (No. Z210013), and ITC-InnoHK Projects at COCHE.

References

1. Banh, D., Kyprianou, I.S., Paquerault, S., Myers, K.J.: Morphology-based three-dimensional segmentation of coronary artery tree from CTA scans. In: Medical Imaging (2007)
2. Bock, S., Giger, M.L., Karssemeijer, N., Kühnel, C., Boskamp, T., Peitgen, H.O.: Robust vessel segmentation. In: Proceedings of SPIE - The International Society for Optical Engineering 2013, pp. 691539–691539-9 (2008)

3. Fu, L., Kang, Y., Zhu, Z.: Centerline correction of incorrectly segmented coronary arteries in CT angiography. Proc. SPIE **8768**, 87683G (2013)
4. Gharleghi, R., et al.: Automated segmentation of normal and diseased coronary arteries - the ASOCA challenge. Comput. Med. Imaging Graph. **97**, 102049 (2022). https://www.sciencedirect.com/science/article/pii/S0895611122000222
5. Gharleghi, R., et al.: Computed tomography coronary angiogram images, annotations and associated data of normal and diseased arteries (2022). https://arxiv.org/abs/2211.01859
6. Han, D., Shim, H., Jeon, B.: Automatic coronary artery segmentation using active search for branches and seemingly disconnected vessel segments from coronary CT angiography. PLoS ONE **11**(8), e0156837 (2016)
7. Han, K., et al.: Reconnection of fragmented parts of coronary arteries using local geometric features in X-ray angiography images (2021)
8. Isensee, F., Jaeger, P.F., Kohl, S.A.A., Petersen, J., Maier-Hein, K.H.: nnU-Net: a self-configuring method for deep learning-based biomedical image segmentation. Nat. Methods **18**(2), 203–211 (2020)
9. Li, M., et al.: Deep learning segmentation and reconstruction for CT of chronic total coronary occlusion. Radiology **306**, 221393 (2022)
10. Li, Q., Tian, J.: Partial shape-preserving splines. Comput. Aided Des. **43**(4), 394–409 (2011)
11. M'Hiri, F., Duong, L., Desrosiers, C., Cheriet, M.: VesselWalker: coronary arteries segmentation using random walks and Hessian-based vesselness filter. In: IEEE International Symposium on Biomedical Imaging (2013)
12. Kerfoot, E., Clough, J., Oksuz, I., Lee, J., King, A.P., Schnabel, J.A.: Left-ventricle quantification using residual U-Net. In: Pop, M., et al. (eds.) STACOM 2018. LNCS, vol. 11395, pp. 371–380. Springer, Cham (2019). https://doi.org/10.1007/978-3-030-12029-0_40
13. Mou, L., Chen, L., Cheng, J., Gu, Z., Zhao, Y., Liu, J.: Dense dilated network with probability regularized walk for vessel detection. IEEE Trans. Med. Imaging **39**(5), 1392–1403 (2019)
14. Mou, L., et al.: CS2-Net: deep learning segmentation of curvilinear structures in medical imaging. Elsevier (2021)
15. Roth, G.A., et al.: Global burden of cardiovascular diseases and risk factors, 1990–2019: update from the GBD 2019 study. J. Am. Coll. Cardiol. **76**, 2982 (2020). (15), 77 (2021)
16. Serruys, P.W., et al.: Coronary computed tomographic angiography for complete assessment of coronary artery disease: JACC state-of-the-art review. J. Am. Coll. Cardiol. **78**(7), 713–736 (2021)
17. Shit, S., et al.: clDICE - a novel topology-preserving loss function for tubular structure segmentation. In: Computer Vision and Pattern Recognition (2021)
18. Wang, Q., et al.: Geometric morphology based irrelevant vessels removal for accurate coronary artery segmentation. In: 2021 IEEE 18th International Symposium on Biomedical Imaging (ISBI), pp. 757–760 (2021)
19. Wolterink, J.M., Leiner, T., Išgum, I.: Graph convolutional networks for coronary artery segmentation in cardiac CT angiography. In: Zhang, D., Zhou, L., Jie, B., Liu, M. (eds.) GLMI 2019. LNCS, vol. 11849, pp. 62–69. Springer, Cham (2019). https://doi.org/10.1007/978-3-030-35817-4_8
20. Zhang, X., et al.: Progressive deep segmentation of coronary artery via hierarchical topology learning. In: International Conference on Medical Image Computing and Computer-Assisted Intervention (2022)

21. Zheng, Y., Wang, B., Hong, Q.: UGAN: semi-supervised medical image segmentation using generative adversarial network. In: 2022 15th International Congress on Image and Signal Processing, BioMedical Engineering and Informatics (CISP-BMEI) (2022)
22. Zhou, Z.H., Feng, J.: Deep forest. Natl. Sci. Rev. **6**(1), 74–86 (2019)
23. Zhu, X., Cheng, Z., Wang, S., Chen, X., Lu, G.: Coronary angiography image segmentation based on PSPNet. Comput. Methods Programs Biomed. **200**(4), 105897 (2020)